Model Risk and Differential Geometry Applied to Sensitivity Analysis

Z. Krajčovičová* & P. P. Pérez Velasco †

*Department of Mathematics, Faculty of Informatics, Campus Elviña s/n, 15071–A Coruña, Spain, z.krajcovicova@udc.es,

† Model Risk Division, Banco Santander, Boadilla del Monte, Spain, pedpperez@gruposantander.com

Abstract. The aim of this contribution is to emphasize the importance of differential geometry within the financial modeling and usage process. The paper aims specifically at encouraging the inclusion of differential geometry to improve on the usage of a given model, and to reduce the inherent model risk Krajčovičová et al. (2018, 2017). The authors exemplify these ideas by considering application to the P&L explanation of digital options with the Black–Scholes model and demonstrate the improvement by comparing results under Euclidean and non–Euclidean geometries.

Key words: model risk, differential geometry, Riemannian manifold, curvature, covariant derivative, Profit and Loss explanation

1 Introduction

The usage of mathematical modeling has long played an important role in understanding the design principle underlying financial markets that are characterized by complex nonlinear dynamical systems. Mathematical models are abstract representations of reality used to describe and predict some aspects of the financial reality with varying levels of detail, and thus are prone to measurement and model uncertainty. Bearing in mind uses of a model and understanding limitations of the underlying assumptions are key when dealing with a model and its outputs.

The model development, implementation and usage often involve assumptions concerning the geometry of the data and model space, setting by default the Euclidean geometry. The assumption of Euclidean geometry is rarely questioned or empirically tested, e.g. inherent in many algorithms is differential calculus that implicitly assumes a metric structure. The computation of gradients, directional derivatives or Hessians of the output function is often required while performing various business applications such as risk and capital allocation, sensitivity analysis or optimization methods (e.g., quadratic programming, least–squared problems or unconstrained optimization). For example, in capital allocation one often considers the effect of a marginal change in the volume of a particular business line on the total capital, or the sensitivity analysis often involves the computation of derivatives of the output function with respect to one or several independent variables.

Acknowledgements and Disclaimer: The authors thank Álvaro Iglesias and Luis Herraiz for providing their knowledge, insight and expertise that greatly assisted the present contribution. Any remaining errors are our own. The views in this paper are solely those of the authors.

This work has been partially funded by EU H2020-MSCA-ITN-2014 (WAKEUPCALL Grant Agreement 643045).

As pointed out by the authors in Krajčovičová et al. (2018), most financial models can be encoded as statistical varieties that capture all assumption regarding the likely nonlinear behavior of the system and the dependencies of the model on the development data. Statistical models can be thought of as a family of parametrized probability distributions that forms a geometric variety, known as the model manifold $\mathcal{M}$ in which model parameters form its coordinate system.

The natural geometric structure of the family of probability distributions is defined by a Riemannian manifold, $\mathcal{M}$, that is determined by two fundamental forms. A Riemannian metric tensor, g, can be viewed as the first fundamental form which aims to compute the intrinsic geometric structure of $\mathcal{M}$, such as geodesics, area and volume. The second fundamental form aims to uncover the extrinsic structure of the manifold relative to the ambient space and is determined by the Riemannian curvature tensor (the second order derivative of vector field on $\mathcal{M}$), where the directional derivative is the Riemannian connection ∇. The Riemannian structure generalizes the Euclidean counterparts by studying smooth manifolds endowed with a smoothly changing metric. When the underlying space of the given problem is nonlinear in nature, the assumption of Euclidean geometry may among other things decrease the accuracy and introduce a bias throughout the computation process.

We propose that the measure of curvature which, in a broad sense, is a measure by which a geometrical object deviates from begin flat, may be used in two contexts. First, it can be seen as a mean to control the inherent model risk.[1] Second, even in the case of a flat underlying model variety, different geometries may better fit the particular usage of a model and so increase the overall performance.

The aim of this paper is to emphasize the importance of the geometry of the underlying space in financial models, focusing on differential computations in the more general context of a Riemannian manifold. The use of the Riemannian geometry allows us to define a measure of distance between sets of parameters in terms of changes in the model structure, rather than changes in the values of the parameters themselves. With some examples of the daily P&L explanation of digital options we show that when the underlying geometry of the space of interest is taken into account, the modeling results are not only more accurate and consistent, but also reduce the potential model risk[2] inherent in the given problem.

The rest of the paper is structured as follows. In Section 2 we summarize the central concepts from Riemannian geometry of our interest and introduce the terminology used throughout the paper. Section 3 presents the main arguments for the consideration of the non–linear structure of the financial models. Section 4 and Section 5 describe the option price sensitivities and the covariant version of the Taylor expansion followed by the daily P&L analysis for the digital option. A choice of an appropriate Riemannian metric is discussed in Section 6 and applied to the example of the P&L introduced in previous section. Section 7 provides some final conclusions and directions for future work. Finally, the Appendix

[1] A Riemannian manifold is an n–dimensional space that near each of its points resembles an n–dimensional Euclidean space. Thus, while locally it looks Euclidean, globally it does not — precisely what happens in the presence of model risk Krajčovičová et al. (2018, 2017).

[2] In the present contribution risk is understood as uncertainty.

contains two more examples of the daily P&L of digital options for a synthetic underlying asset and a volatility equity index.

2 GEOMETRICAL BACKGROUND

In what follows, we introduce some standard elements of the differential calculus on the manifold to emphasize which geometrical concepts are of our particular interest, and also to fix the terminology and notation. For a more detailed exposition we refer the reader to Do Carmo (1992).

We assume that the manifold under consideration, $\mathcal{M}$, is always sufficiently smooth, and so can be endowed with a Riemanian metric, $g = \big(g_{ij}\big)$, i.e. smoothly varying inner product on the tangent space. Riemannian manifolds locally resemble an Euclidean space meaning that up to first order they look like Euclidean spaces. Differences arise when we study the second order approximation to these spaces which suffices to recover all the information encoded in the Riemannian manifold, Nicolaescu (2009). To proceed with a dynamic analysis, we need to be able to differentiate a vector field along a curve with the use of a notion of affine connection.

Given a Riemannian manifold $(\mathcal{M}, g)$, the fundamental theorem of Riemannian geometry states that there exists a unique linear connection ∇_g on $\mathcal{M}$, called the Levi–Civita connection (of g) that preserve the metric ($\nabla_g g = 0$) and is torsion–free. [3] This connection is determined in a local coordinate system through the Christoffel symbols: $\nabla_{\partial_i}\partial_j = \Gamma^k_{ij}\partial_k$. With these conventions, the covariant derivative of the coordinates v^i of a vector field is $v^i_{;j} = (\nabla_j v)^i = \partial_j v^i + \Gamma^i_{jk} v^k$.

The connection defines the correspondence between vectors in different tangent spaces of the manifold. Note that the rate of change of the tangent space defines the geometry of the manifold. The actual rate of change of a vector field X on the manifold is the change of X along some coordinate curve γ, plus the change of the coordinate curve itself. Therefore, we have

$$\frac{DX^i}{d\gamma^i} = \frac{\partial X^i(\gamma)}{\partial \gamma^j} + \Gamma^i_{jk} X^k(\gamma).$$

If $(U, x^1, \ldots, x^n)$ is a coordinate chart on $\mathcal{M}$, then the Christofell symbols Γ^k_{ij} of the Levi–Civita connection are related to the functions g_{ij} by the formulas

$$\Gamma^k_{ij} = \sum_l \frac{1}{2} g^{kl}\Big(\frac{\partial g_{li}}{\partial x^j} + \frac{\partial g_{lj}}{\partial x^i} - \frac{\partial g_{ij}}{\partial x^l}\Big), \tag{2.1}$$

while the curvature R has components

$$R^l_{ijk} = \frac{\partial \Gamma^l_{ki}}{\partial x^j} - \frac{\partial \Gamma^l_{ji}}{\partial x^k} + \Gamma^r_{ki}\Gamma^l_{jr} - \Gamma^r_{ji}\Gamma^l_{kr}\ .$$

The curvature tensor is a function which describes the degree to which the manifold deviates from being a flat Euclidean space. The curvature is defined in terms of the intrinsic geometry of a surface and gives rise to changes in acceleration,

[3] The torsion free condition on the connection is given by $[X, Y] = \nabla_X Y - \nabla_Y X$, where $[X, Y]$ is the Lie bracket of the vector fields X and Y.

which is mathematically described by the affine connection. For any smooth function $f : \mathcal{M} \to \mathbb{R}$ we then obtain the second covariant derivative (see Shima et al. (1997)) given by

$$\nabla_g^2 f = \Big(\frac{\partial^2 f}{\partial x^i \partial x^j} - \Gamma_{ij}^k \frac{\partial f}{\partial x^k} \Big) dx^i \otimes dx^j.$$

With notation as above, we next introduce the coordinate free version of the covariant Taylor series that can be further used to learn how vectors, 1–forms and higher rank tensors move along the manifold. For a function f defined on a Riemannian manifold, a second–order approximation of f around a point $p \in \mathcal{M}$ is given by

$$\begin{aligned} f(q) &= f(p) + \big\langle grad\, f, v \big\rangle_p + \frac{1}{2} \big\langle Hess\, f(p)[v], v \big\rangle_p + O(t^3) \\ &= f(p) + \big\langle grad\, f, v \big\rangle_p + \frac{1}{2} \big\langle \nabla_{X(p)} grad\, f(p), v \big\rangle_p + O(t^3) \end{aligned}$$

where $v \in T_p\mathcal{M}$. Note that every term of the Taylor expansion is a tensor. The covariant Taylor approximation is robust to local re–parametrization Mukherjee et al. (2010) of the model which comes from the fact that the Riemannian distance is a measure of how the probability density function changes, regardless on how it was parametrized.

3 NEED TO CONSIDER NONLINEAR STRUCTURES

The principles of sensitivity analysis have a wide range of applications in finance, e.g. in various stages of the model development process, model usage, validation, or as a part of different methodologies and strategies. Sensitivity analysis is often computed either via the linearization of the model parameters, by analyzing the system mean behavior, by using simulations for approximating finite differences of system outputs or by other sensitivity measures. The chosen method often depends upon assumptions and the amount of information required from the analysis, and they range in both complexity and fundamental understanding.

Performing a proper sensitivity analysis is challenging for many types of financial models, particularly for those that are highly dimensional and whose nonlinear dynamics induce a very strong nonlinear dependence structure in the underlying probability distribution. These models may exhibit widely varying parameter values that can even change depending on the dynamic behavior of the model and, thus, can vary dramatically in different parts of the parameter space.

A possible explanation for this changing behavior may be the underlying nonlinear manifold structure, in particular the mathematical relationship between the parameters and the states, but it may equally well be caused by the inherent model risk, for example, by measurement uncertainty of the data, due to inaccurate calibration strategies, model mis–specification or even improper usage. On top of that, the varying behavior may just be a result of a mismatch between the underlying geometry of the space and the canonical Euclidean geometry that is often, implicitly or explicitly, assumed for the model. If this is the case, this source of model risk can be overcome by formulating the sensitivities directly on the underlying space with a proper inner product.

Furthermore, the covariant differentiation of section of a vector bundle which is a generalization of the standard differentiation of a function, can be used to encode properties of the financial market system, like fluctuations and to make the difference between points depend on the neighborhood. This means that the relation between points would to some extend be described by the market behavior.

Essential to sensitivity analysis is the vector calculus with notions such as gradient, divergence, partial derivative or Laplacian. In this case, the varying behavior plays a key role, particularly when exploring larger regions of the nonlinear underlying model space, where the standard methods that rely on Euclidean geometry may fail or perform poorly at best. These concepts can be replaced by the generalized covariant differentiation defined on the Riemannian manifolds —-crucial when working in curved spaces— in order to consider the local geometry of the underlying Riemannian space.

Differential geometry seems particularly well suited to exploit the natural representation of the underlying model space as a Riemanian manifold, as it may make use of the local information for sensitivity analysis. This way the curvature of the model manifold, which is directly defined by the parameters of the underlying model describing its dynamic behavior, can be taken into account. The effects of model risk can then be assessed by comparing the Taylor expansion with its covariant version. So, the covariant Taylor expansion will converge in the absence of model risk but also in its presence (provided that we work in sufficiently small region of the given variety).

4 Option Price Sensitivities

In this section we start by briefly reviewing the theory of option pricing, recalling the basic concepts and fixing notation in passing. For more information see Hirsa et al. (2013); Hull et al. (2016).

A contingent T–claim, for $T \geq 0$, is an $\mathcal{F}_T$ measurable random variable $Y \geq 0$, see Korn et al. (2001). The arbitrage free price V_t of Y at time $0 \leq r \leq T$ is given by[4]

$$V_t = \mathbb{E}\left[\exp\Big(- \int_t^T r_u du\Big) Y \,\Big|\, \mathcal{F}_t \right], \tag{4.1}$$

where the expectation is taken with respect to the risk neutral probability measure p of the discounted cash flow. Since the option price is an expectation of some random variable Y, where Y can be written as a function of the stock price at maturity, the sensitivities of interest are given by the partial derivatives with respect to the corresponding parameter, $\partial V/\partial \theta^i$.

For the rest of the paper we consider that the price of the underlying security follows the Black–Scholes (BS) model, i.e. its price under the equivalent martingale measure satisfies

$$S_t = S_0 \exp\left(\left(r - \frac{\sigma^2}{2} \right) t + \sigma \sqrt{t} W_t \right)$$

[4] To simplify notation we shall at times omit the subscript 't' in V_t.

at any time $t \geq 0$, where $S_0 > 0$ and $\sigma > 0$ denotes the initial price and the volatility, respectively, and W_t is a Brownian motion, refer to Hull et al. (2016). Thus, S_t follows a log–normal distribution with density

$$p(S|\mu,\sigma) = \frac{1}{\sqrt{2\pi}\sigma} exp\left(- \frac{(\log S - \mu)^2}{2\sigma^2} \right), \quad \mu = \log S_0 + \left(r - \frac{\sigma^2}{2}\right)t. \tag{4.2}$$

The second order Taylor expansion of the option price V_t is then given by

$$\begin{aligned} dV \approx \frac{\partial V}{\partial t}dt + \frac{\partial V}{\partial S}dS + \frac{\partial V}{\partial \sigma}d\sigma + \frac{\partial V}{\partial r}dr + \frac{1}{2}\left(\frac{\partial^2 V}{\partial S^2}dS^2 + \frac{\partial^2 V}{\partial \sigma^2}d\sigma^2 + \frac{\partial^2 V}{\partial r^2}dr^2 + \frac{\partial^2 V}{\partial t^2}dt^2 \right) \\ + \frac{\partial^2 V}{\partial S \partial \sigma}dSd\sigma + \frac{\partial^2 V}{\partial S \partial r}dSdr + \frac{\partial^2 V}{\partial r \partial \sigma}drd\sigma + \textbf{error}. \end{aligned} \tag{4.3}$$

The Taylor expansion is mainly used to relate sensitivities to the market value for derivative instruments and to revalue the market price (profit and loss, P&L, further addressed in Sec. 5). From a geometrical perspective, the standard Taylor expansion is calculated under the Euclidean geometry of the data and the model. The key for our argument is to realize that, similarly as for many other financial models, the underlying hypothesis of the option pricing is encoded as a statistical model that captures all assumptions regarding the likely nonlinear behavior of the system and the dependencies of the model on the development data, see Krajčovičová et al. (2018, 2017).

For example, in the case of BS, the statistical model represents a family of log–normal probability distributions that forms a curved statistical manifold $\mathcal{M}$ with coordinates μ and σ (refer to eq. 4.2). A point on $\mathcal{M}$, determined by (μ_i, σ_i), denotes a specific probability distribution $p(x|\mu_i, \sigma_i)$ defined on the Euclidean data space, $\mathcal{X}$. The option price V refers to a functional over $\mathcal{M}$, and so the underlying geometrical structure of $\mathcal{M}$ induces a Riemannian structure also on the corresponding option model space. For more details see Krajčovičová et al. (2018).

A distinction can be made between two types of sensitivities. First, the sensitivities of the option price with respect to variations in market variables such as variations in time or in price of the underlying which measure the risk exposure (e.g., Theta, Delta, Gamma). Second, the sensitivities of the option value with respect to changes in the model parameters (e.g., Rho, Vega, Volga). Besides, these different types of sensitivities can be seen as various movements on two diverse underlying spaces. Derivatives with respect to the market factors refer to changes in the flat $\mathcal{X}$ for a point on $\mathcal{M}$, i.e. for a given $p(x|\mu, \sigma)$, whereas sensitivities with respect to model parameters, i.e. μ and σ, pertain to changes and movements across the potentially curved space of models $\mathcal{M}$. The curved geometry of the underlying model variety implies that the standard differential calculus should be modified according to the inherent local geometry by considering covariant differentiation.

The covariant differential of a function along a tangent vector v for a given connection ∇ that determines the curvature of the underlying space, written $\nabla_v V$, is simply $dV(v)$. In specific coordinate system, the i–th component of ∇V is $\partial V/\partial\theta^i$ which is just the standard partial derivative. The ij–th component of the second differential $\nabla^2 V$ is given by

$$\left(\nabla^2 V\right)_{(ij)} = \frac{\partial^2 V}{\partial\theta^i \partial\theta^j} - \sum_k \Gamma_{ij}^k \frac{\partial V}{\partial\theta^k},$$

where Γ_{ij}^{k} are the Christoffel symbols of the corresponding connection defined as in eq. 2.1.

To reduce potential model risks we suggest to modify the second and higher–order greeks[5] with respect to model parameters by correction in the curvature of the underlying space. The second–order covariant Taylor expansion of the option price that accounts for the underlying model structure can then be written

$$\begin{aligned} dV \approx & \frac{\partial V}{\partial t}dt + \frac{\partial V}{\partial S}dS + \frac{\partial V}{\partial \sigma}d\sigma + \frac{\partial V}{\partial r}dr + \frac{1}{2}\frac{\partial^2 V}{\partial S^2}(dS)^2 + \frac{1}{2}\frac{\partial^2 V}{\partial t^2}dt^2 + \frac{\partial^2 V}{\partial S \partial \sigma}dSd\sigma + \frac{\partial^2 V}{\partial S \partial r}dSdr \\ & + \frac{\partial^2 V}{\partial r \partial \sigma}drd\sigma + \frac{1}{2}\left(\frac{\partial^2 V}{\partial \sigma^2}d\sigma^2 - \mathbf{\Gamma}^{\sigma}_{\sigma\sigma}\frac{\partial \mathbf{V}}{\partial \sigma} - \mathbf{\Gamma}^{\mathbf{r}}_{\sigma\sigma}\frac{\partial \mathbf{V}}{\partial \mathbf{r}} + \frac{\partial^2 V}{\partial r^2}dr^2 - \mathbf{\Gamma}^{\sigma}_{\mathbf{rr}}\frac{\partial \mathbf{V}}{\partial \sigma} - \mathbf{\Gamma}^{\mathbf{r}}_{\mathbf{rr}}\frac{\partial \mathbf{V}}{\partial \mathbf{r}}\right) + \text{error} \qquad (4.4) \\ & \approx \text{Euclidean Taylor expansion} + \text{Curvature correction} + \text{residuals}. \end{aligned}$$

By comparing the Taylor expansion given by eq. 4.3 with its covariant alternative, we can notice that in the case of the Euclidean geometry the curvature terms vanish. On the other hand, if $\mathcal{M}$ is not flat the significance of the curvature corrections in eq. 4.4, depending on the specific application, may become relevant. Since a Riemannian manifold is locally Euclidean, within a small neighborhood and for directions with a small curvature, the curvature terms may often be neglected. However, for larger curvatures or neighborhoods, it is necessary to explicitly compute the curvature terms if only to show that they are indeed negligible.

The argumentation outlined above and a consideration of the limitations of the flat geometry when applied to financial markets suggest the introduction of a Riemannian geometry in the model manifold $\mathcal{M}$. Considering the geometry of the problem may open new modelling possibilities due to the introduction of a new modeling degree of freedom.

5 Daily P&L analysis for Digital options under the Black–Scholes model

In this section we emphasize the importance of the curvature in the presence of model risk on the daily P&L analysis for a digital option under the BS model.

Digital options are among the most popular types of exotic options traded over–the–counter (OTC) on stocks, stock indices, foreign currencies, commodities and interest rates. Models used in banks to value these payoffs are more complex in order to better simulate the smile profile for each component of the underlying.

However, there is no generally accepted model for pricing exotic FX options to market. The use of not only different models but also of different methodologies, results in widely dispersed model–dependent exotic option prices for any given set of market and contract inputs. Model risk is especially acute in the case of OTC exotic options for which the daily traded closing mark–to–market prices do not exist, so they need to be mark–to–model instead. Given that models are used throughout the price–making process, from pricing to identifying hedging strategies, calculating daily P&L,

[5] Option price sensitivities or option factor sensitivities are approximations used to determine the change in price of the option due to a change in the value of one of the inputs or model parameters, commonly called greeks. Refer to Hull et al. (2016) for more details.

defining risk limits, reporting to key stakeholders internally and externally, model risk is an important consideration in the OTC exotic option market.

To highlight model risk we choose the BS model due to its known limitations and drawbacks to price digital options, consequently when used for the P&L explanation.[6] The motivations for this are twofold. First, while using the BS model we can focus on the issue of model misspecification. Second, with the choice of this model we can address the link between curvature and the inherent model risk.

In general, more complex models are usually hard to calibrate. Some market practitioners, therefore, tend to stick to the BS constant–volatility model to price exotic options, but they also adopt some rules of thumb, based on hedging arguments, to include the volatility smile/skew or market frictions into the pricing and hedging. We show that enhancements of the BS model approach can be performed through changes in the curvature of $\mathcal{M}$ for a properly selected Riemannian metric. In the end, the choice of a particular model is always a trade–off between accuracy and simplicity.

For the sake of completion, we first briefly review some material on the valuation of a standard digital option. Full details can be found e.g. in Laurence (2017). For a digital option with European exercise, pricing is relatively straightforward as a closed–form expression is available in the BS framework. For the European digital call option that pays off 1 at expiration T if the underlying S_T is over the strike K, the payoff at maturity is

$$D(K) = \begin{cases} 1 & \text{if } S_T \geq K \\ 0 & \text{if } S_T < K, \end{cases}$$

where S_T is the underlying value at maturity. In a risk neutral world, the price of an option can be determined by integrating over the range of possible price outcomes as given by eq. 4.1, and so for the digital option we have

$$D(K) = e^{-rT} \int_K^\infty p(S) dS,$$

where r is the risk free rate and $p(S)$ is the probability density function. With log–normally distribution prices, $\log(S)$ has a normal distribution with μ given in eq. 4.2 and standard deviation $\sigma\sqrt{T}$. Expressed in terms of the cumulative probability, the digital call option price is

$$D(K) = e^{-rT}\mathbb{P}\big[S_T \geq K\big] = e^{-rT}\mathbb{P}\big[\log(S_T) \geq \log(K)\big] = e^{-rT}\mathcal{N}(d_2),$$

where $\mathcal{N}(\cdot)$ is the standard normal cumulative function and d_2 is given by

$$d_2 = \frac{\ln\left(\frac{S_0}{K}\right) + \left(r - \frac{\sigma^2}{2}\right)T}{\sigma\sqrt{T}}.$$

To value this discontinuous payoff, one possible market consensus is to use a piecewise linearization, by valuing a combination of vanilla calls on the underlying asset. The linearized payoff is equivalent to a call spread: long $1/\epsilon$ calls

[6] Note that the same approach outlined in this paper can be used for other models such as local or stochastic volatility models.

with strike $(K-\epsilon)$ and short $1/\epsilon$ calls with strike K. [7] The calls have the same expiration date as the digital with final payoff $1/\epsilon \cdot \max\big(S_T-(K-\epsilon),0\big)-1/\epsilon \cdot \max\big(S_T-K,0\big)$, where the factor ϵ is chosen by the trader. The payoff of the digital call can be thought of as a limit of a call spread

$$D(K)=\lim_{\epsilon\to 0}\frac{1}{\epsilon}\Big(C(K-\epsilon)-C(K)\Big)=-\frac{\partial C(K)}{\partial K}.$$

We examine the BS model when applied for the P&L explanation. The P&L analysis provides users with a coherent breakdown of the drivers of P&L movements between two points in time with reference to a selected number of pricing factors. Most of the methodologies for P&L analysis essentially involve performing an approximation of the portfolio using a Taylor expansion of the change in the value metric in terms of the risk factors which are defined as instantaneous stresses or parallel shocks and thus rely on the first and higher–order sensitivities of the assets in the portfolios.

The P&L explanation comes with challenges owing to the complexities of derivative instruments. This approach works very well for simple derivatives (or linear) products that are explained by the main greeks of the model. Yet, this becomes more complicated with larger market moves and more exotic products, besides the inherent model uncertainty of the model used. [8] Even though mathematically European digital options are easy to price, computing accurate greeks is quite difficult as the model assumptions and in particular the model distribution can dramatically change their values through the life of an option.

In general, there are two fundamental differences between digital options and standard vanilla options: mixed convexity and discontinuous payoffs. The convexity of the digital option changes sign depending on whether it is in–the–money or out–of–the–money. Besides, with time approaching the expiry date, the sensitivities to certain risk factors change their behavior making the option very difficult to hedge. Another source of model risk arises from the usage of the call spread which becomes apparent in the case of unexpected and sudden shifts. The main risk however arises when the underlying price oscillates around the strike price near expiration. This may lead to unexpected, strong variations of the risk exposure of the banks, especially for second order–exposures like Gamma or Volga.

The behavior of some of the option sensitivities with respect to the position of the current price of the underlying or the time to expiration suggests to link this effect to the curvature of the underlying space. Higher–order sensitivities compare information in two different states (points on the underlying model space) and so distance indicates the difference between them. If this difference is characterized only based on the Euclidean geometry, some of the background information may be lost and the result may not fit the practical significance of the financial analysis but rather cause deviations. Geometrically, the space would not be flat but curved, and the curvature would change depending on the different factors influencing the dynamic behavior of the option price during its life.

[7] A call spread can be selected by choosing the smallest spread which results in a position size considered small enough to be liquid, either by representing a real possibility for purchase in the market or by being representable in the firm's risk reports by delta positions that can be achieved with reasonable liquidity.

[8] For example, since mispricing of the BS model for out–of–money options is large, the performance is strongly affected by the extent to which theoretical model characteristics or market data (skew/smile) are taken into account in their implementation.

To illustrate this point we apply our proposal to a portfolio V consisting of a single digital call option priced under the BS model.[9] In order to explain the potential factors that may influence the changes in the portfolio over a given period we decompose the daily P&L of the portfolio using a second order Taylor expansion. The daily P&L for the digital option with the underlying local geometry of the model space with coordinate system (μ, σ), given market data, can be calculated as

$$\begin{aligned} dV_t = V_t - V_{t-1} \approx & \frac{\partial V}{\partial t}dt + \frac{\partial V}{\partial S}dS + \frac{\partial V}{\partial \sigma}d\sigma + \frac{\partial V}{\partial r}dr + \frac{1}{2}\frac{\partial^2 V}{\partial S^2}dS^2 + \frac{1}{2}\frac{\partial^2 V}{\partial \sigma \partial S}d\sigma dS \\ & + \frac{1}{2}\left(\frac{\partial^2 V}{\partial \sigma^2} - \Gamma^r_{\sigma\sigma}\frac{\partial V}{\partial r} - \Gamma^\sigma_{\sigma\sigma}\frac{\partial V}{\partial \sigma}\right)d\sigma^2 + \frac{1}{2}\left(\frac{\partial^2 V}{\partial r^2} - \Gamma^r_{rr}\frac{\partial V}{\partial r} - \Gamma^\sigma_{rr}\frac{\partial V}{\partial \sigma}\right)dr^2 \\ & + \underbrace{\left(\frac{\partial^2 \mathbf{V}}{\partial \mathbf{r}\partial\sigma} - \mathbf{\Gamma}^{\mathbf{r}}_{\mathbf{r}\sigma}\frac{\partial \mathbf{V}}{\partial \mathbf{r}} - \mathbf{\Gamma}^{\sigma}_{\mathbf{r}\sigma}\frac{\partial \mathbf{V}}{\partial \sigma}\right)\mathbf{dr}d\sigma + \frac{\partial^2 V}{\partial t^2}dt^2}_{\text{Not included since it is negligible}} + \textbf{residuals} \\ \approx & \text{ Euclidean Taylor expansion} + \text{Curvature correction} + \textbf{residuals}, \end{aligned}$$

where correction terms are with respect to the curvature of the underlying space, S_t is the underlying, t is the time to expiration, σ is the volatility and r is interest rate respectively. [10]

First we calculate the P&L under the assumption of Euclidean geometry and then compare its daily approximation errors with the one rising from the P&L under certain curved geometry. Using this approach, we can analyze and evaluate the impact of the model risk on the performance of the Taylor approximation. We consider a simple digital call written on the USD/CAD exchange rate in which the institution pays on 24th June 2017, the strike $K = 1.325$ being fixed on 24th June 2016 ($T = 1$) for the initial price of the underlying at $S_0 = 1.282$. The time evolution of the underlying with the realized volatility and interest rate are depicted in Fig. 5.1. To illustrate the proposed approach we further consider other underlying assets whose results are included in the Appendix.

We start by considering the P&L explanation as done usually in practice, under the Euclidean geometry, i.e. all Christoffel symbols are equal to zero, $\Gamma^k_{ij} = 0$. In general the P&L attribution will, as with most analysis of surplus processes, leave some unexplained amounts. The error (unexplained part) under the Euclidean geometry is depicted in Fig. 5.2. We present the total error which is just the difference between the market at time t and the theoretical P&L calculated using the Taylor expansion one day before t, i.e. $(P\&L - Theoretical\, P\&L)$.

[9] Digital options that might be part of a widely diversified portfolio are in some cases approached and examined in an isolated manner, especially in those cases where the underlying is threatening to finish close to the strike and the difficulty in its management increases.

[10] Usually the effect of the interest rate sensitivity is limited and included in the residual term as well as other higher–order derivatives. The effect of interest rate shifts are usually less important than those of other factors, most notably the price and volatility of the underlying instrument. For these derivatives a single sensitivity to a parallel shift in yield curve usually suffices — this is ρ. To illustrate our approach we include also the second differential with respect to the movement of the interest rate since this may become relevant for longer lived options. Refer to Fig. 6.2.

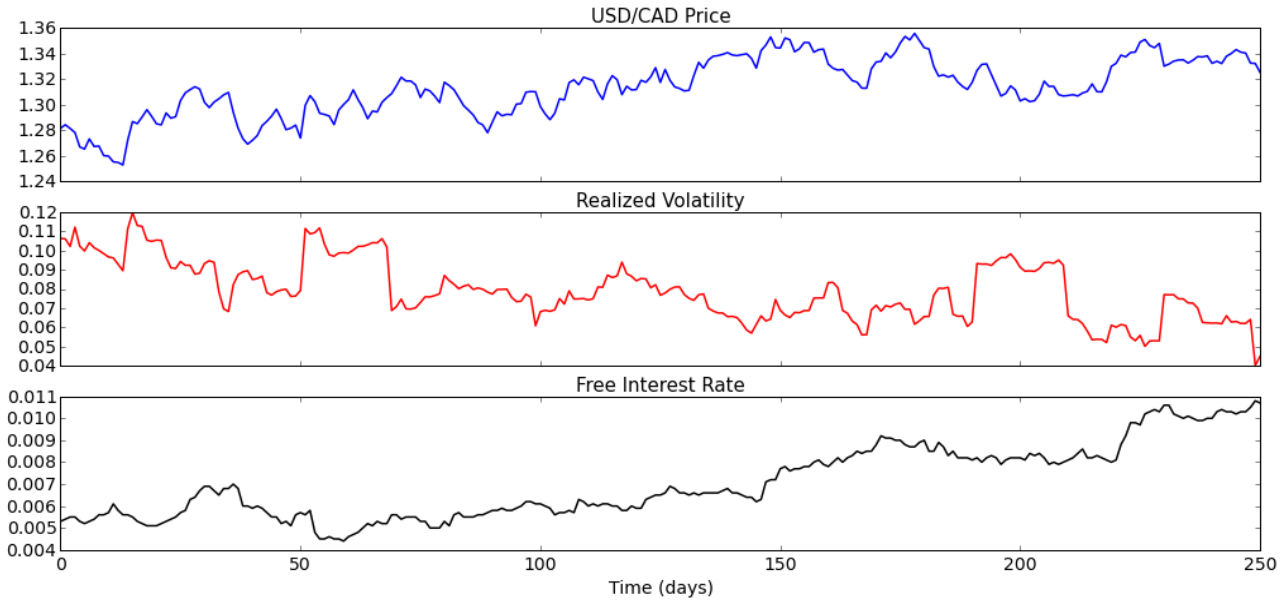

Fig. 5.1. Evolution of the underlying USD/CAD exchange rate with the realized volatility and interest rate ($r = r_d - r_f$).

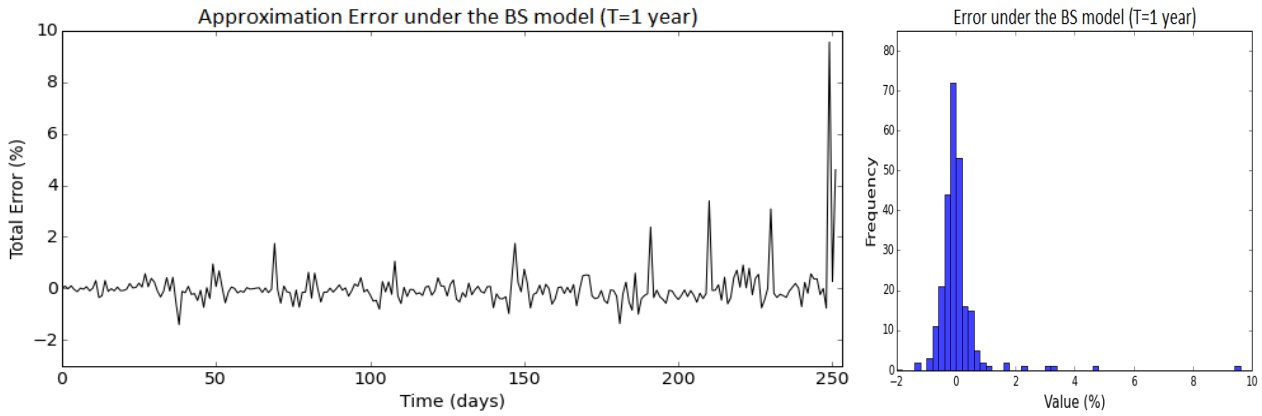

Fig. 5.2. Total errors under the BS model with the assumption of Euclidean geometry and total P&L of 0.043. The initial price of the underlying asset is given by $S_0 = 1.28166$ and $S_T = 1.33263$ at expiry with fixed $K = 1.325$. Descriptive statistics for errors: mean = 0.000017, std. dev. = 0.0084, skew = 6.93.

Generally speaking, the main goal of the theoretical P&L is to perfectly explain the dynamics of the option price. The key thing here is that the P&L always exhibit variance so the fact that the errors are not identically zero is not of particular importance in itself when it comes to P&L explanation.[11] Rather one has to consider other characteristics of the errors and define an acceptable deviation representing the difference between the actual movements of the option price and the movement implied by a given linear combination of the risk factors. Deviations, among others, arise due to the following issues: model limitations (changes in data not been mapped to any of the risk factors or actual shape of movements), higher–order terms in Taylor expansion not quantified, or inconsistent usage of the model with the underlying assumptions.

According to Figs. 5.1 and 5.2, the closer to expiry the larger the approximation errors. Besides it can be seen that the errors were sensitive to changes in the stock price, the realized volatility and also the interest rates. The explanation of these results is in line with the theory and the variance in daily errors can be linked to the deviations of the BS limitations, such as not taking into account jumps in volatility or in price, from the real market behavior. As the BS model is a good approximation to market reality in *static* situations, the second–order approximation assuming an underlying Euclidean geometry stays meaningfully close to the option price for small variations in price and volatility.

Most errors do not exceed 1% in absolute value, but can be of up to 10%. This means that in this particular case the largest fraction of daily errors which correspond to no jumps is small in absolute values, whereas for jump events the error in the BS model is largely affected.

6 CHOICE OF A RIEMANNIAN METRIC

One of the basic questions is to determine the geometrical structure, in particular to define a Riemannian metric and an affine connection on the corresponding statistical manifold which would appropriately reflect the dynamical behaviour of the model, the underlying S_t, the payoff and the market data. Any smooth manifold will admit a large family of Riemannian metrics which may display diverse geometrical properties. Goodness of the metric depends on its ability to encode second–order information about the problem. Different descriptions of the space give rise to different families of metrics, and hence to different natural geometries.

For the sensitivity analysis that explores the underlying model space locally, it may be advantageous to consider different geometries of the underlying space each having different properties that may be of benefit in different forms of analysis and specific applications. For example, the motivating requirement for asymmetry in statistical inference is captured in the preferred point metric and associated geometry (see Critchley et al. (1993)), whereas an assessment of the conditional variance of a maximum likelihood estimator is performed by the observed Fisher–Rao information matrix (see Efron (1975)). Another possibility is to extract a proper metric from the observed data to examine the dynamic

[11] For example, frequency of the rebalancing: In theory, the model assumes continuous dynamics and so requires continuous trading which is not feasible in practice (e.g. transaction costs or market incompleteness).

behaviour of the model with respect to the behavior of the financial market.

6.1 Fisher–Rao information metric

As mentioned in Sec. 3, the underlying space for a digital option is a statistical manifold possessing a Riemannian structure which can be endorsed with the Fisher–Rao information metric, see Rao (1987). For the parametric density $p(\theta)$, the Fisher–Rao information matrix is given by $g = \mathbb{E}_\theta[\nabla_\theta l(\theta) \cdot \nabla_\theta l(\theta)^T]$ where $l(\theta) = \log p(\theta)$ is the log–likelihood function, ∇ is the gradient of the log–likelihood at θ (implicitly depending on $\mathcal{X}$) and $\mathbb{E}_\theta$ denotes expectation taken with respect to $p(\theta)$.

Amari Amari (1985) showed that a wide range of metrics for comparing probabilities reduce to a simple function of the Fisher–Rao metric when the density functions are close to each other. Examples of such metrics include Kullback–Leiber (KL), Bhattarcharrya, Matusita–Hellinger or Jensen–Shannon divergence. KL divergence, also known as information gain or relative entropy, is a non–symmetric measure of the difference between two probability distributions p and q, but it is also a measure of the expected number of extra bits required to code samples from p when using a code based on q. [12] Moreover, it is also known that the KL divergence is the Riemannian distance under the Levi–Civita connection, refer to Amari (1985) again, with the approximation being valid up to second order terms. The minimization of the KL divergence is equivalent to maximum–likelihood estimation, i.e. maximizing the likelihood of data under our estimate is equal to minimizing the difference between our estimate and the real data distribution.
The explicit form of the Fisher–Rao metric for the family of log–normal distributions is:

$$g\big(r(t),\sigma(t)\big) = \begin{bmatrix} g_{rr} & g_{r\sigma} \\ g_{\sigma r} & g_{\sigma\sigma} \end{bmatrix} = \begin{bmatrix} \dfrac{1}{\sigma(t)^2} & 0 \\ 0 & \dfrac{2}{\sigma(t)^2} \end{bmatrix}$$

and the Christoffel symbols of the second kind associated with the Levi–Civita connection are:

$$\Gamma^r = \begin{bmatrix} \Gamma^r_{rr} & \Gamma^r_{r\sigma} \\ \Gamma^r_{r\sigma} & \Gamma^r_{\sigma\sigma} \end{bmatrix} = \begin{bmatrix} 0 & -\dfrac{1}{\sigma(t)} \\ -\dfrac{1}{\sigma(t)} & 0 \end{bmatrix}, \quad \Gamma^\sigma_{ij} = \begin{bmatrix} \Gamma^\sigma_{rr} & \Gamma^\sigma_{r\sigma} \\ \Gamma^\sigma_{r\sigma} & \Gamma^\sigma_{\sigma\sigma} \end{bmatrix} = \begin{bmatrix} \dfrac{1}{2\sigma(t)} & 0 \\ 0 & -\dfrac{1}{\sigma(t)} \end{bmatrix}.$$

It is well known Said et al. (2017) that, after a change of coordinates, the length element ds^2 coincide with the length element of the Poincaré half–space model of hyperbolic geometry. This means that the underlying space when equipped with its Fisher–Rao information metric becomes a space of constant negative curvature. The covariant version of the

[12] See Amari (1985) for a proof that the KL divergence between two infinitesimally close distributions is half of the square of their Riemannian distance:

$$D_{KL}\big(p(x|\theta) \,\|\, p(x|\theta + d\theta)\big) \approx \frac{1}{2} g_{ij} d\theta^i d\theta^j.$$

second–order derivatives is

$$\nabla_g^2 V_{\sigma\sigma} = \frac{\partial^2 V}{\partial \sigma^2} - \Gamma_{\sigma\sigma}^{\sigma}\frac{\partial V}{\partial \sigma} - \Gamma_{\sigma\sigma}^{r}\frac{\partial V}{\partial r} = \frac{\partial^2 V}{\partial \sigma^2} + \frac{\mathbf{1}}{\sigma}\frac{\partial \mathbf{V}}{\partial \sigma},$$

$$\nabla_g^2 V_{rr} = \frac{\partial^2 V}{\partial r^2} - \Gamma_{rr}^{\sigma}\frac{\partial V}{\partial \sigma} - \Gamma_{rr}^{r}\frac{\partial V}{\partial r} = \frac{\partial^2 V}{\partial r^2} - \frac{\mathbf{1}}{\mathbf{2}\sigma}\frac{\partial \mathbf{V}}{\partial \sigma}.$$

Figures 6.1 and 6.2 show that the correction under the negatively curved geometry induced by the Fisher–Rao information metric mainly affects the second order derivative with respect to volatility.

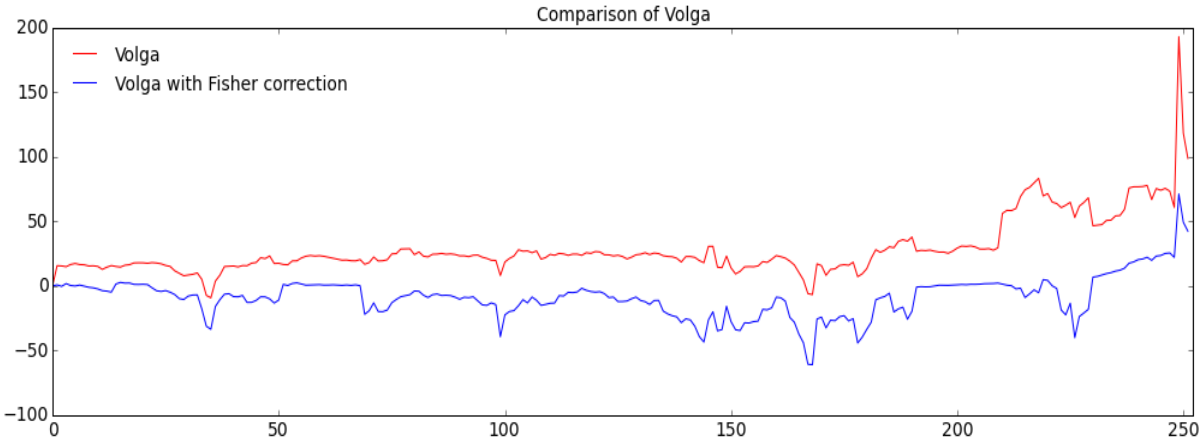

Fig. 6.1. Change in the second order derivatives with respect to σ, $\dfrac{\partial^2 V}{\partial \sigma^2}$.

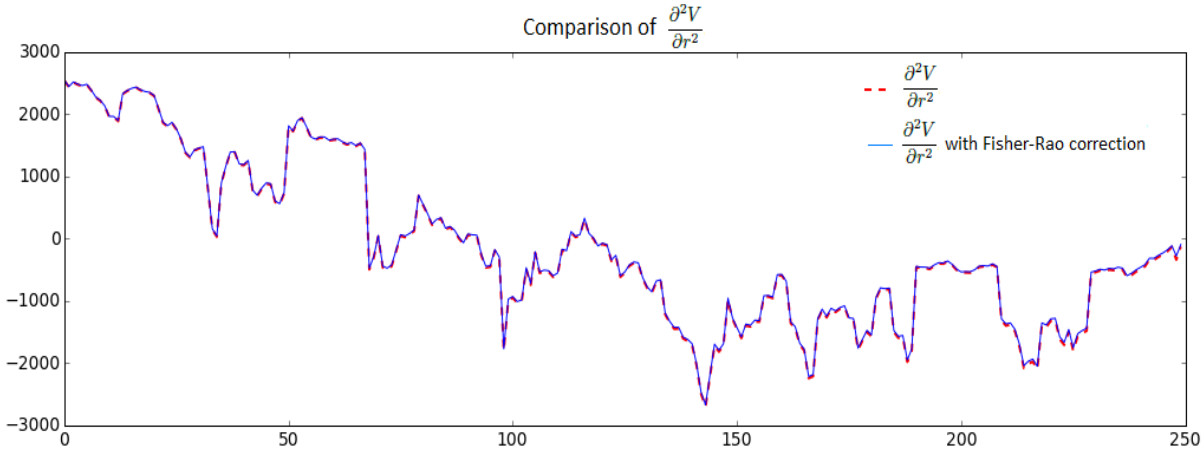

Fig. 6.2. Change in the second–order derivatives with respect to r, $\dfrac{\partial^2 V}{\partial r^2}$.

The resulting daily approximation errors under the Fisher–Rao geometry are shown in Fig. 6.3. In comparison with Fig. 5.2, Fig. 6.3 illustrates the decrease in approximation errors, especially around the maturity, with mean -0.054%. Correcting for the nonlinearities implied by the changing volatility decreases the extreme errors and increases the number of errors around zero, i.e. the overall performance of the P&L approximation is improved.

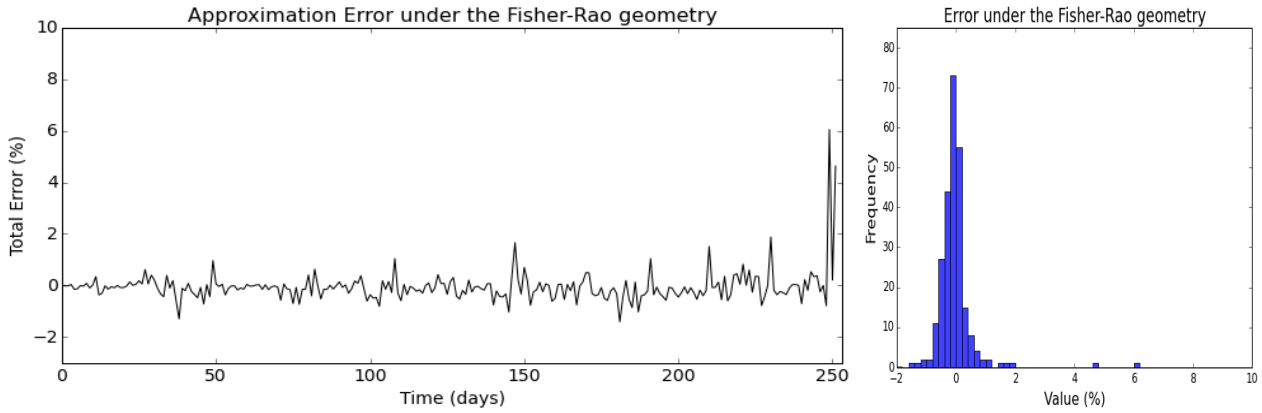

Fig. 6.3. Total errors under the Fisher–Rao geometry. The initial price of the underlying asset is given by $S_0 = 1.28166$ and $S_T = 1.33263$ at expiry with fixed $K = 1.325$. Descriptive statistics: mean = -0.054%, std. dev. = 0.0063, skew = 5.42.

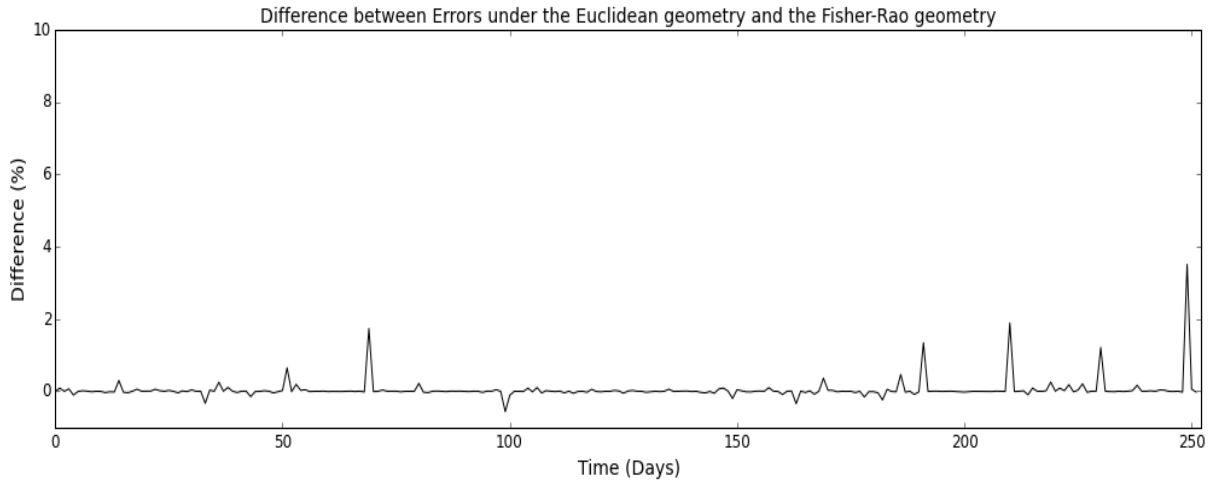

Fig. 6.4. Difference between the absolute approximation errors under the Euclidean geometry and the Riemannian geometry associated with the Fisher–Rao information metric, i.e. $Total_t = (|Error_{Euclidean}| - |Error_{Fisher}|)_t$.

Figure 6.4 compares the absolute approximation errors under the Euclidean geometry and the geometry induced by the Fisher–Rao information metric. Large positive values represent large improvements of the Fisher–Rao metric.

The almost absence of negative values means that Fisher–Rao rarely worsens the calculations. Values close to zero mean either that the error is small in both cases or that there is almost no improvement. Thus, we can notice an overall improvement in the approximation. The correction for the model risk changes with respect to the dynamics implied by the model, particularly variations in the volatility of the underlying, with considerable enhancement during larger shifts in data.

6.2 Christoffel symbols based on critical points of digital options

The Fisher geometry seems a natural choice if all we know is the underlying statistical family of the given model. The risks involved in trading digital options are, however, not directly related only to the underlying asset. The main risk arises when the price of the underlying oscillates around the strike (barrier) near expiration. In general, the discontinuity in the payoff will make Gamma or Vega flip sign at the barrier. Delta and Gamma magnitudes attain maximum around the barrier and the closer to expiry the higher the magnitude of these risks. Moreover these sensitivities become large as $t \to T$ for $S \approx e^{-(r-q)t}K$. Additionally, given the mixed convexity of the second derivatives, the impacts of large up or down movements are not symmetric, so direction matters.

Considering general characteristics specific to digital contracts or the particular usage of the model, it may be possible to choose a geometry that is better suited for the given problem.[13] Tuning the geometry of the variety with respect to some of the influencing factors of the given contract such as moneyness, distance to barrier (current value of the state variable) or time to maturity of the option, may improve the overall P&L explanation power when compared to the Euclidean or Fisher–Rao metrics.

Defining a metric is not an intuitive task. Metrics are defined in terms of a local inner product and it may be difficult to understand the implications of a specific choice on the resulting geometry. Alternatively, we may consider to determine directly the curvature of the manifold through the Christoffel symbols for a given connection.[14] Considering the time to maturity (different behavior closer to expiry), distance to K and the direction of the changes in volatility, interest rates and stock price, we propose to use the Christoffel symbols given in Table 1, where the constants, a_{it} and b_{it} for $i = 1, 2, 3, 4$ are fitted for this particular example.[15] In this particular example, the constants take the values shown in Table 1.

The Christoffel symbols, and so the curvature adjustments, depend both on the parameters that define the underlying probability distribution, such as volatility and interest rate, but also factors that characterize the given digital contract,

[13] Note that the choice of a geometry is problem dependent, i.e. following the same idea other geometries can be derived for various families of contracts such as barrier or Bermuda options, or that are better suited for other applications such as hedging.

[14] The curvature of the manifold is determined by the connection that is defined by the Christoffel symbols. Thus we can directly work with the Christoffel symbols.

[15] Note that this choice is only a first attempt, the existence and the construction of a covariant derivative that would be theoretically consistent with the P&L explanation for certain underlying assets and contracts and that will outperform the standard techniques is left for further research. See Sec. 7.

Christoffel symbols	**for** $S_t < Ke^{-r_t t}$ **and** $t < \frac{1}{2}T$	**otherwise**	a_{it}	b_{it}
Γ^r_{rr}	$a_{1t}\frac{1}{r_t\sigma_t}$	$b_{1t}\frac{1}{r_t\sigma_t}$	0.7	$-sign(Ke^{-r_t t} - S_t)$
$\Gamma^\sigma_{\sigma\sigma}$	$a_{2t}\frac{1}{\sigma_t}$	$b_{2t}\frac{1}{\sigma_t}$	$0.6 \cdot sign(\sigma_t - \sigma_{t-1})$	$2 \cdot sign(Ke^{-r_t t} - S_t)$
$\Gamma^r_{\sigma\sigma}$	$a_{3t}\frac{r_t}{\sigma_t^2}$	$b_{3t}\frac{r_t}{\sigma_t^2}$	$-5 \cdot sign(\sigma_t - \sigma_{t-1})$	$-sign(Ke^{-r_t t} - S_t)$
Γ^σ_{rr}	$a_{4t}\frac{1}{r_t\sigma_t^2}$	$b_{4t}\frac{1}{r_t\sigma_t}$	-1.4	-0.25

Table 1. Christoffel symbols fitted to the data: Estimated geometry.

e.g. changing behavior closer to expiration, the importance of the direction of the movement. These are local, thus capturing local variations.

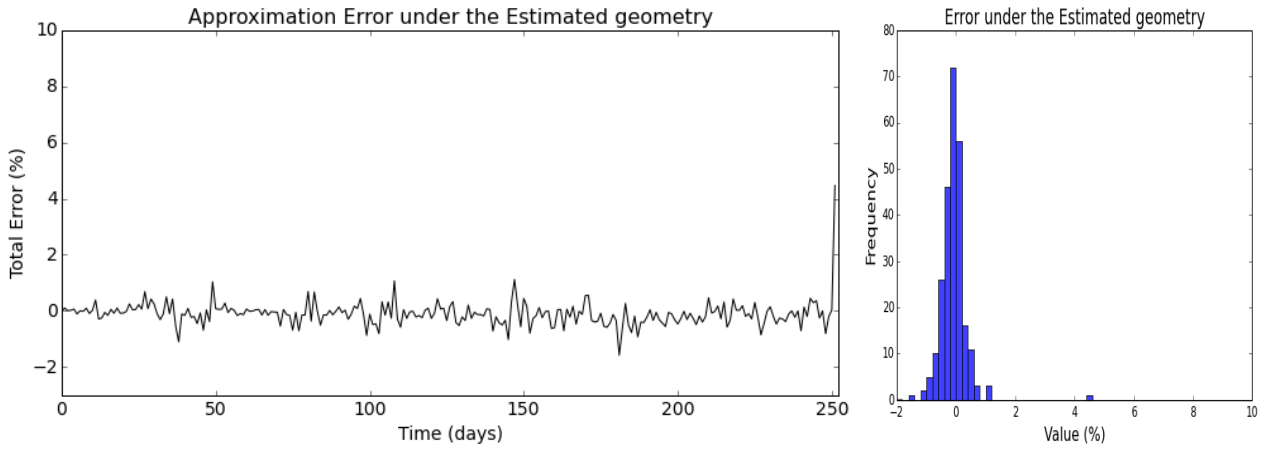

Fig. 6.5. Total approximation errors under the Estimated geometry. The initial price of the underlying asset is given by $S_0 = 1.28166$ and $S_T = 1.33263$ at expiry with fixed $K = 1.325$. Descriptive statistics: mean = -0.09%, std. dev. = 0.0084, skew = 4.015.

As Figs. 6.5 and 6.6 indicate, tuning the curvature towards more specific characteristics of the digital option shows some improvement in the approximation. Figure 6.6 compares the Estimated geometry with the Euclidean and the Fisher–Rao geometries. As positive values represent the decrease in errors induced by the Estimated geometry and negative values mean worsening, we can conclude that the overall performance is enhanced also with respect to the geometry induced by the Fisher–Rao information metric. The curvature expression reveals the following behaviour of the model: with increasing volatility the model risk inherent in the P&L explanation under the BS model increases, exactly when the curvature of the underlying model space plays a crucial role.

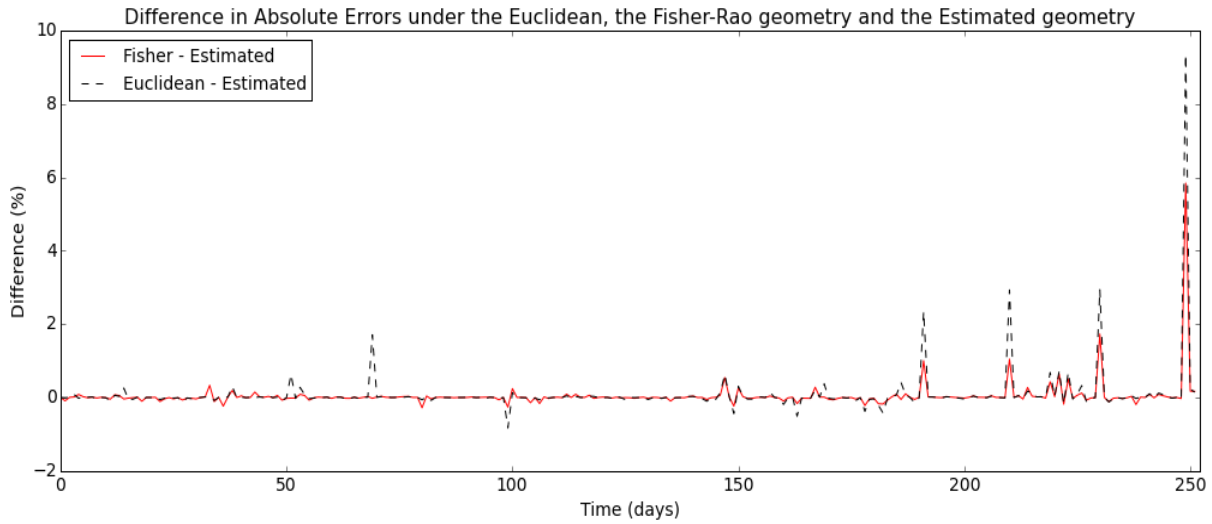

Fig. 6.6. Difference between the absolute approximation errors under the Euclidean geometry, the Riemannian geometry associated with the Fisher–Rao information metric and the Estimated geometry, i.e. $(Fisher - Estimated)_t = (|Error_{Fisher}| - |Error_{Estimated}|)_t$ and $(Euclidean - Estimated)_t = (|Error_{Euclidean}| - |Error_{Estimated}|)_t$.

7 Conclusions and Further Research

The broad aim of the present contribution is to encourage the inclusion of differential geometry to improve on the usage of a given model; equivalently, to reduce the inherent model risk which is inextricably related to its use (linking with Krajčovičová et al. (2018, 2017)). The authors have shown that considering a proper non–Euclidean geometry for the underlying model variety may improve the overall model performance.

The authors have tried to achieve the aforementioned objectives by selecting a widespread and problematic model, payoff and usage: P&L explanation of digital options via the Black–Scholes model. Not only several underlying and market conditions have been assessed but also curved and flat geometries.

This study is of a starting–point nature, suggesting many directions for further research. We would like to highlight the following:

1. Since curvature is affected by the choice of a particular family of models, their usage as well as data, it might be interesting to explore calibration algorithms for selecting most appropriate Riemannian metrics.
2. Choice of a proper metric for other usages besides the P&L explanation or sensitivity analysis (where the differential calculus is applied) and also to other data, models and their associated usages.
3. Of utmost interest in our opinion is to perform theoretical analysis to asses, among others, when improvements are expected and to what order, to identify areas when model risk is amplified or to improve the detection of model failures. In other words, to establish a deeper link with quantification of model risk and model validation.

Bibliography

Amari, S. I. (1985). Differential–geometrical methods in statistics. *Lecture Notes on Statistics, 28*, 1.

Do Carmo, M. P. (1992). Riemannian geometry. *Birkhauser*.

Critchley, F., Marriott, P., & Salmon, M. (1993). Preferred point geometry and statistical manifolds. *The Annals of Statistics*, 1197-1224.

Efron, B. (1975). Defining the curvature of a statistical problem (with applications to second order efficiency).*The Annals of Statistics*, 1189-1242.

Heston, S. L. (1993). A closed–form solution for options with stochastic volatility with applications to bond and currency options. *The review of financial studies, 6(2)*, 327-343.

Hirsa, A., & Neftci, S. N. (2013). An introduction to the mathematics of financial derivatives. *Academic Press.*

Hull, J. C., & Basu, S. (2016). Options, futures, and other derivatives. *Pearson Education India.*

Korn, R., & Korn, E. (2001). Option pricing and portfolio optimization: modern methods of financial mathematics (Vol. 31). *American Mathematical Soc.*.

Krajčovičová, Z., Pérez Velasco, & P.P., Vázques, C. (2018). A New Approach to Quantification of Model Risk for Practitioners. *Under Peer–review*

Krajčovičová, Z., Pérez Velasco, P. P., & Vázques, C. (2017, November). Quantification of Model Risk: Data Uncertainty. *In International Conference on Geometric Science of Information. Springer, Cham,* 523-531.

Laurence, P. (2017). Quantitative Modeling of Derivative Securities: From Theory To Practice. *Routledge*.

Mukherjee, S., Wu, Q., & Zhou, D. X. (2010). Learning gradients on manifolds. *Bernoulli*, 181-207.

Nicolaescu, L. I. (2009). Lectures on the Geometry of Manifolds.

Rao, C. R. (1987). Differential metrics in probability spaces. *Differential geometry in statistical inference, 10*, 217-240.

Said, S., Bombrun, L., & Berthoumieu, Y. (2017). Warped Riemannian metrics for location-scale models. *arXiv preprint arXiv:1707.07163.*

Shima, H., & Yagi, K. (1997). Geometry of Hessian manifolds. *Differential Geometry and its Applications, 7(3)*, 277-290.

8 APPENDIX

We present two other applications for the daily P&L explanation of digital options written on a synthetic underlying asset following a Heston model and on an actual equity index (volatility index VIX). In both examples we examine the impact of the curvature of the underlying variety (model space) on the P&L explanation under the BS model. Based on the results in subsequent subsections, we can conclude that introduction of curvature improves the usage of a given model and equivalently reduces the inherent model risk.

8.1 Digital Option on synthetic underlying asset following Heston model

The aim of this example is to examine the effect of the curvature when the dynamics of the underlying asset resemble the properties that are assumed by the BS model. Under the BS model, the volatility and interest rate are assumed to be at most time dependent, which is not enough in many situations. We consider an underlying asset simulated by the Heston model plus an interest rate following the Vasicek mode, see eqs. 8.1 and 8.2 below. The parameters of these models are set so that the dynamics of the underlying asset moves towards the assumptions of the BS model, i.e. small volatility of volatility and volatility of interest rate (see Fig. 8.1).

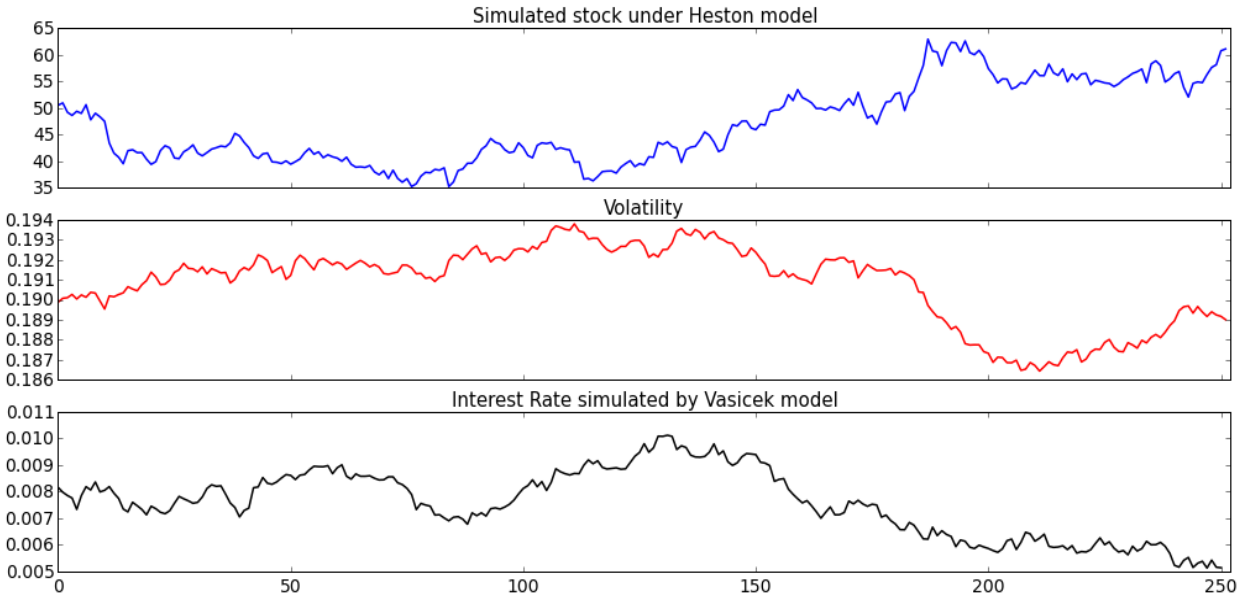

Fig. 8.1. Evolution of the simulated underlying asset with its volatility by the Heston model and the interest rate by the Vasicek model ($S_0 = 50.54, S_T = 61.11, K = 65$; parameters for the Vasicek model: $r_0 = 0.01, \alpha = 0.13, \beta = 0.02, \sigma = 0.005$ and parameters of Heston model: $v_t = 0.188, \bar{v}_t = 0.01, \lambda = 0.01, \rho = -0.2174, \eta = 0.21$).

The Heston model assumes that the asset price and its volatility follow some random processes, refer to Heston (1993). The stochastic process of the asset price S_t is log–normally distributed and the stochastic volatility is assumed

to follow a positive increasing function of a mean–reversion process. The asset dynamics are given by

$$dS_t = \mu S_t dt + \sqrt{v_t} S_t dW_{1,t} \tag{8.1}$$
$$dv_t = -\lambda(v_t - \bar{v})dt + \eta\sqrt{v_t} dW_{2,t}$$

with $\langle dW_{1,t}, dW_{2,t}\rangle = \rho dt$, where μ is the drift and the instantaneous variance of the stock price v_t itself is a stochastic process. λ is the speed of reversion of v_t to its long–term mean $\bar{v}$. We can think of λ as the rate at which the variance reverts back to its long term average value. η is the volatility of the variance process v_t (often called the volatility of volatility). $W_{1,t}$ and $W_{2,t}$ are two dependent Wiener processes with correlation coefficient ρ.

We consider that the interest rate follows the Vasicek model, an Ornstein–Uhlenbeck process whose dynamics are given by the following SDE:

$$dr_t = \alpha(\beta - r_t)dt + \sigma dW_t, \quad r_{t_0} = r_0 \tag{8.2}$$

where $\alpha, \beta > 0$, and σ are constants, and W_t is a Wiener process under the risk neutral measure modelling the random market risk factor and is assumed to be independent from $W_{1,t}$ and $W_{2,t}$. The long term mean is given by $-\alpha/\beta$.

The evolution of the underlying price, its volatility and interest rate are shown in Fig. 8.1. Compared to the evolution of the foreign exchange rate given in Fig.5.1, the simulated asset dynamics, as expected, are not subject to any large price, volatility or interest rate movements (jumps), and so resemble assumptions under the BS model.

The daily approximation errors of the second order Taylor expansion under the Euclidean geometry are depicted in Fig. 8.2. As Fig. 8.2 illustrates, the second–order approximation under the Euclidean structure stays meaningfully close to the option price for small variations in price, volatility and interest rate. As expected, there is a higher variation closer to expiration and when the asset price oscillates around strike. These factors are not taken into account in the sensitivities based on the BS model and so in this situations the model incorporates high model risk since it is used in areas for which it was not developed.

Figures 8.3, 8.4, 8.5 and 8.6 illustrate the average improvement of the covariant Taylor expansion for the daily P&L explanation of a digital option under the Fisher–Rao geometry and the Estimated geometry in comparison with errors under the Euclidean geometry. In comparison with the evolution of the approximation errors for the exchange rate given in Figures 6.3 and 6.4 under the Fisher–Rao geometry and Figures 6.5 and 6.6 under the Estimated geometry we can see that the curvature corrections are rather small. This is in line with the theoretical assumptions, since the BS model is assumed to be a good approximation of the market reality in static situations or in a equilibrium state on the financial market.

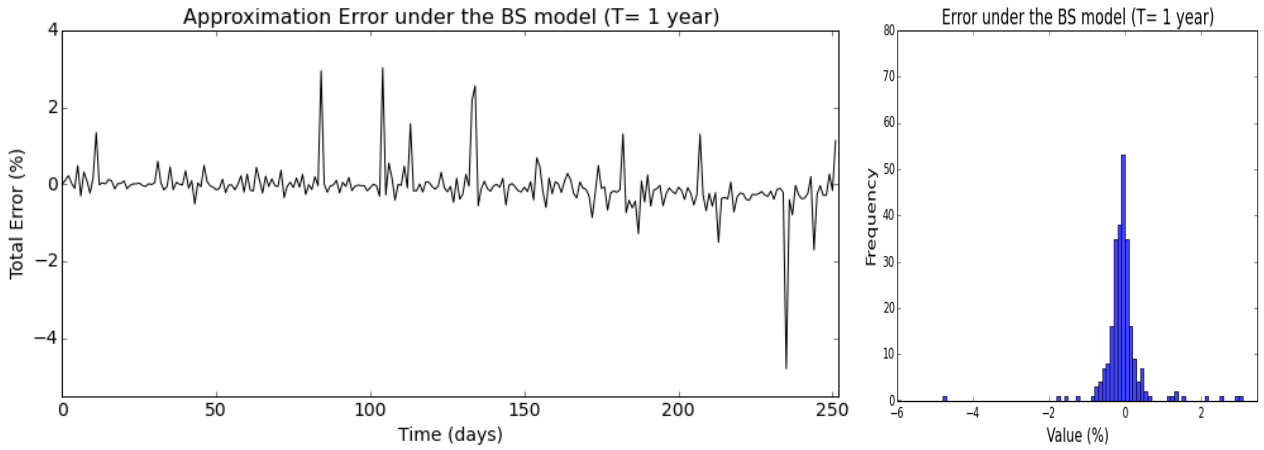

Fig. 8.2. Total approximation errors under the Euclidean geometry. The initial price of the underlying asset is given by $S_0 = 50.54$ and at expiry $S_T = 61.11$ with fixed $K = 65$. Descriptive statistics: mean = -0.0058%, std. dev. = 0.006, skew = -0.367.

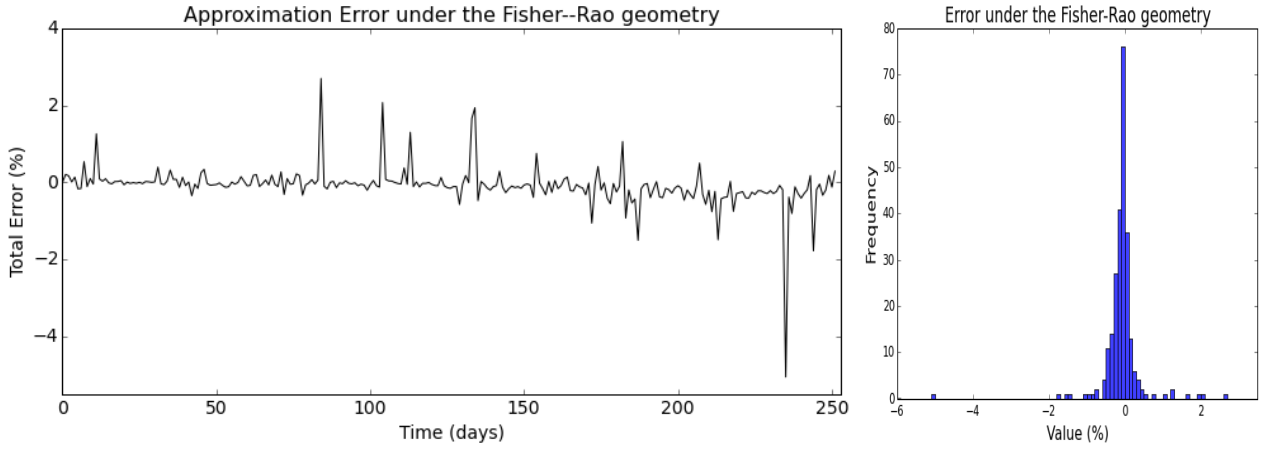

Fig. 8.3. Total approximation errors under the Fisher–Rao geometry. The initial price of the underlying asset is given by $S_0 = 50.54$ and $S_T = 61.11$ at expiry with fixed $K = 65$. Descriptive statistics: mean = -0.086%, std. dev. = 0.0052, skew = -2.37.

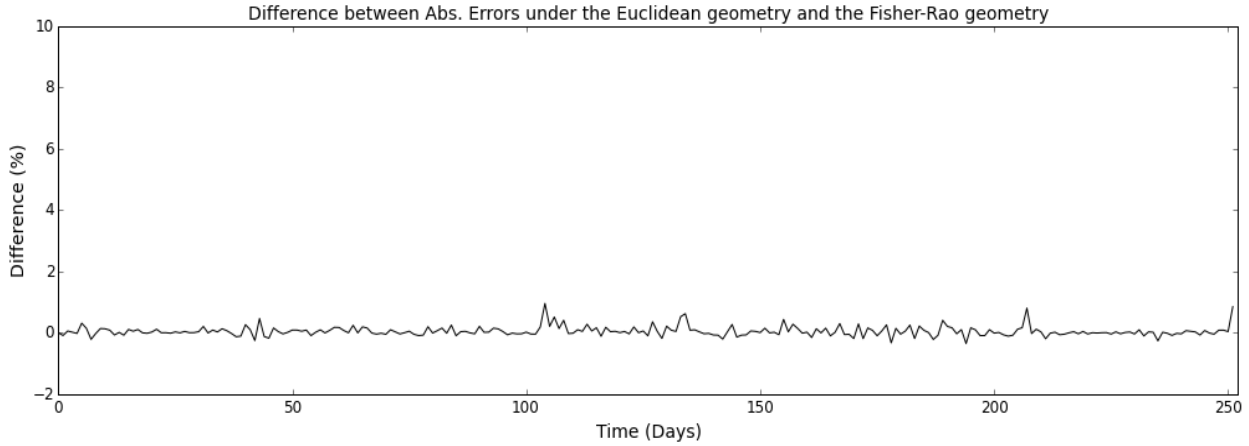

Fig. 8.4. Difference between the absolute approximation errors under the Euclidean geometry and the Riemannian geometry associated with the Fisher–Rao information metric. The initial price of the underlying asset is given by $S_0 = 50.54$ and $S_T = 61.11$ at expiry with fixed $K = 65$.

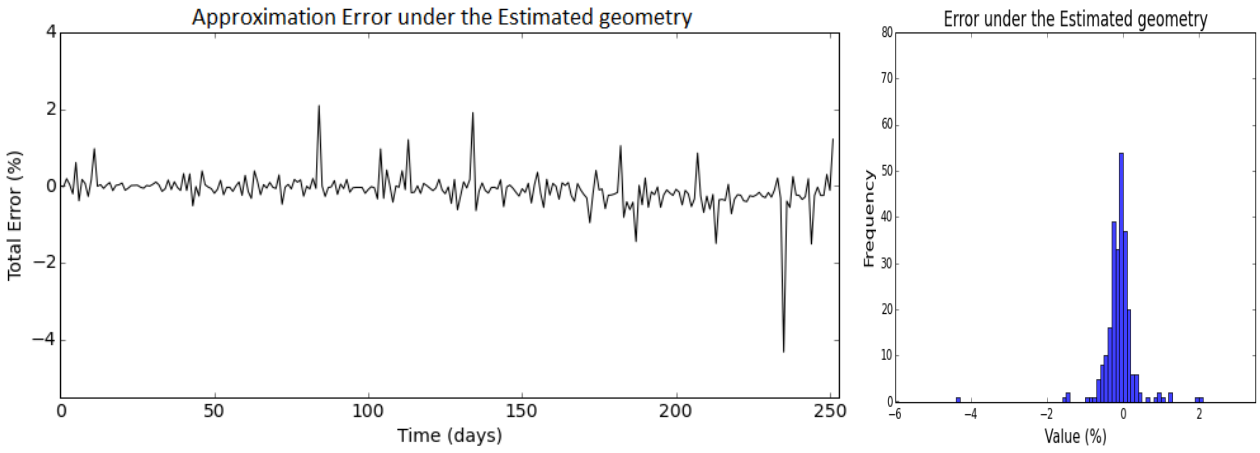

Fig. 8.5. Total approximation errors under the Estimated geometry. The initial price of the underlying asset is given by $S_0 = 50.54$ and $S_T = 61.11$ at expiry with fixed $K = 65$. Descriptive statistics: mean = -0.10%, std. dev. = 0.0046, skew = -2.3.

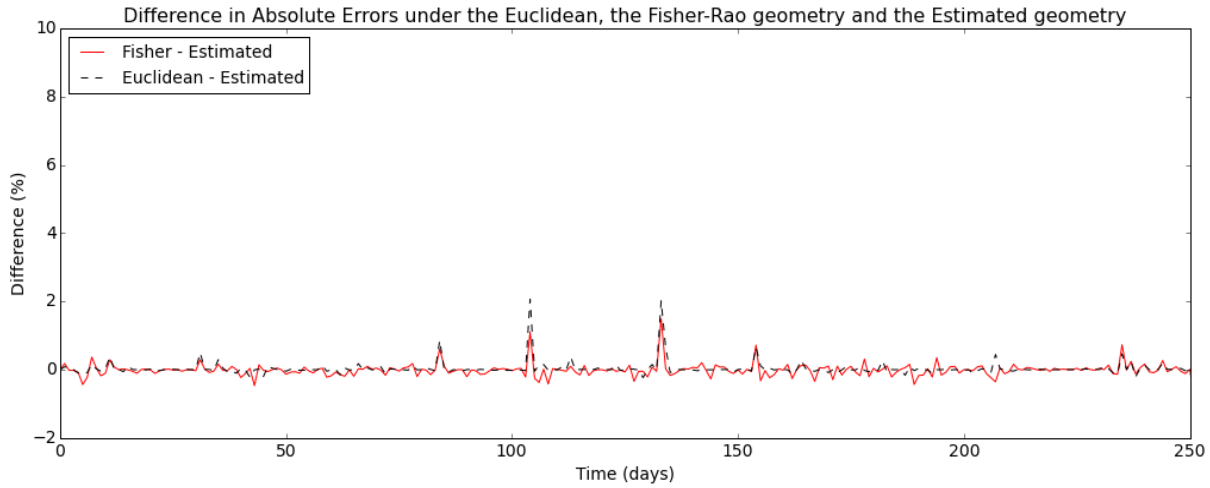

Fig. 8.6. Difference between the approximation error under the Euclidean geometry and the Estimated geometry. The initial price of the underlying asset is given by $S_0 = 50.54$ and $S_T = 61.11$ at expiry with fixed $K = 65$.

8.2 Digital Option on Volatility Index on Equity

We consider the P&L explanation for a digital option on the volatility index VIX in which the institution pays on $3rd$ January 2018, the strike $K = 13$ being fixed on $4th$ January 2017 $(T = 1)$ for the initial price $S_0 = 11.85$. The time evolution of the underlying with the realized volatility and interest rate are depicted in Fig. 8.7.

The daily approximation errors under the Euclidean geometry are depicted in Fig. 8.8. As can be seen, there is a relation between the errors and the daily volatility and price changes, bigger changes mean bigger approximation errors. The largest fraction of daily errors is small in absolute value as they refer to small variations in price and volatility.

In Figures 8.9, 8.10, 8.11 and 8.12 we illustrate the average improvement of the covariant Taylor expansion for daily P&L explanation of a digital option by comparing the Taylor expansion with the Euclidean geometry, the Fisher–Rao geometry and the Estimated geometry. Whereas negative values in Figs. 8.10 and 8.12 mean deterioration of the approximation, positive values represent the decrease in daily errors and so improvement in the P&L explanation, we can conclude that overall performance is enhanced by the Fisher–Rao information metric and even more by the Estimated geometry. Thus, accounting for a proper geometry of the underlying model variety may significantly improve the usage of the model.

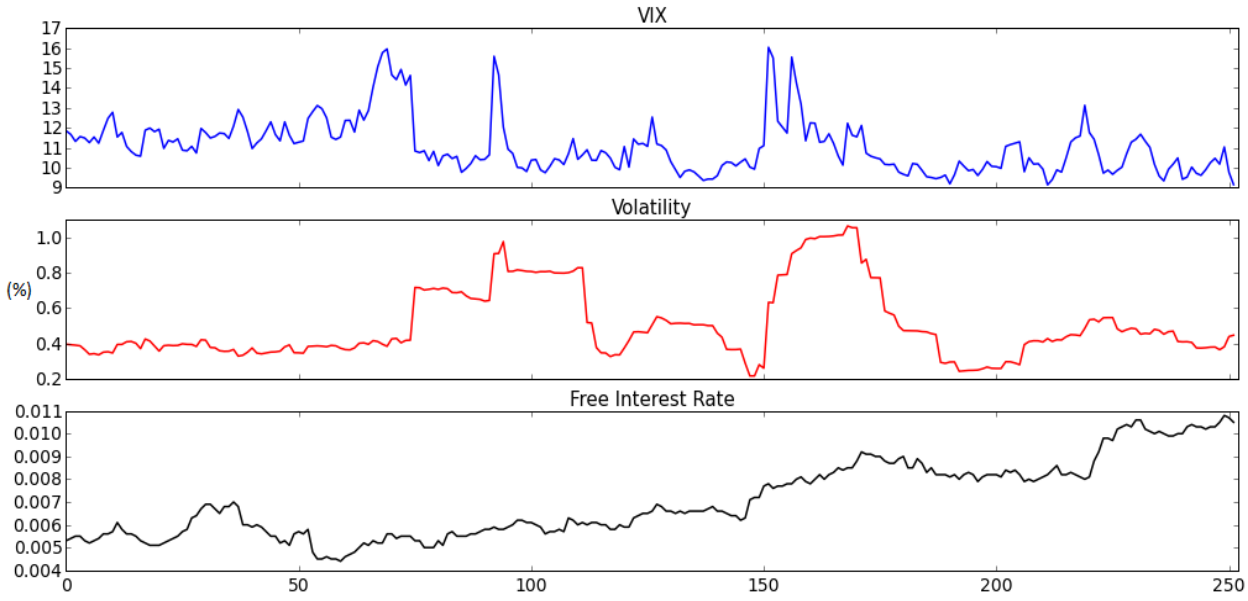

Fig. 8.7. Evolution of the underlying VIX volatility index with the realized volatility and interest rate.

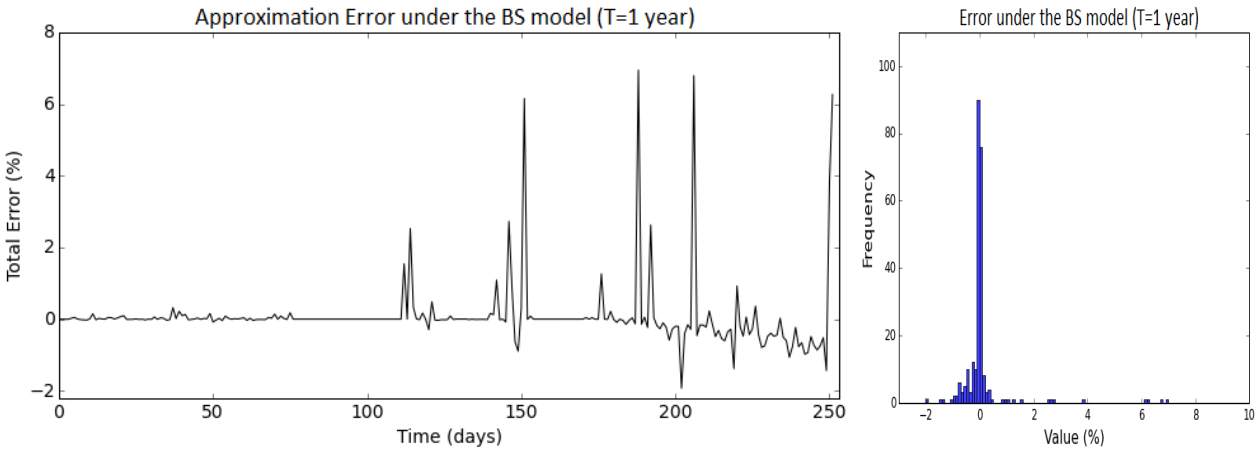

Fig. 8.8. Total approximation errors under the Euclidean geometry. The initial price of the underlying asset is given by $S_0 = 11.85$ and $S_T = 9.15$ at expiry with fixed $K = 13$. Descriptive statistics: mean = 0.075%, std. dev. = 0.0097, skew = 5.15.

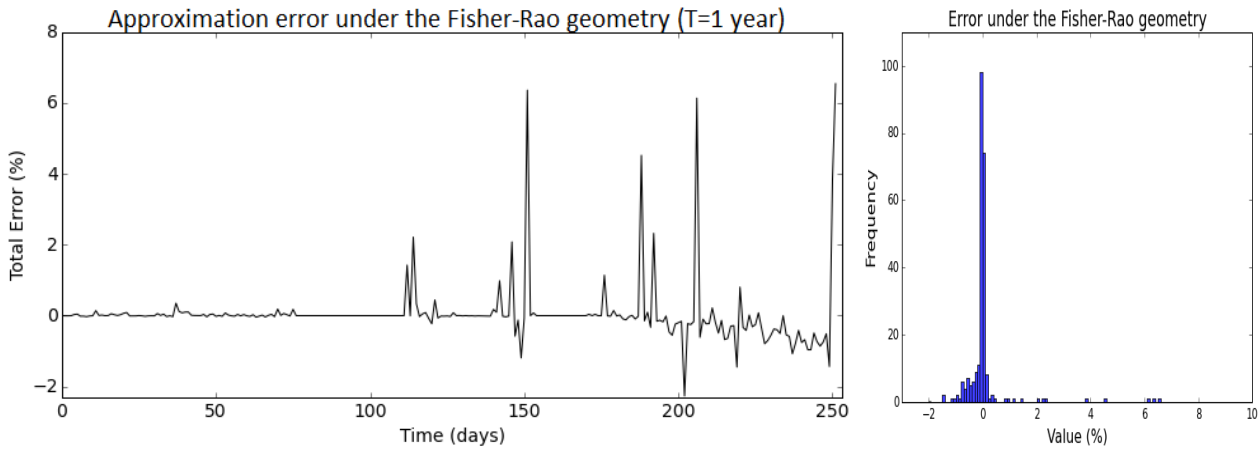

Fig. 8.9. Total approximation errors under the Fisher–Rao geometry. The initial price of the underlying asset is given by $S_0 = 11.85$ and $S_T = 9.15$ at expiry with fixed $K = 13$. Descriptive statistics: mean = 0.047%, std. dev. = 0.0089, skew = 5.038.

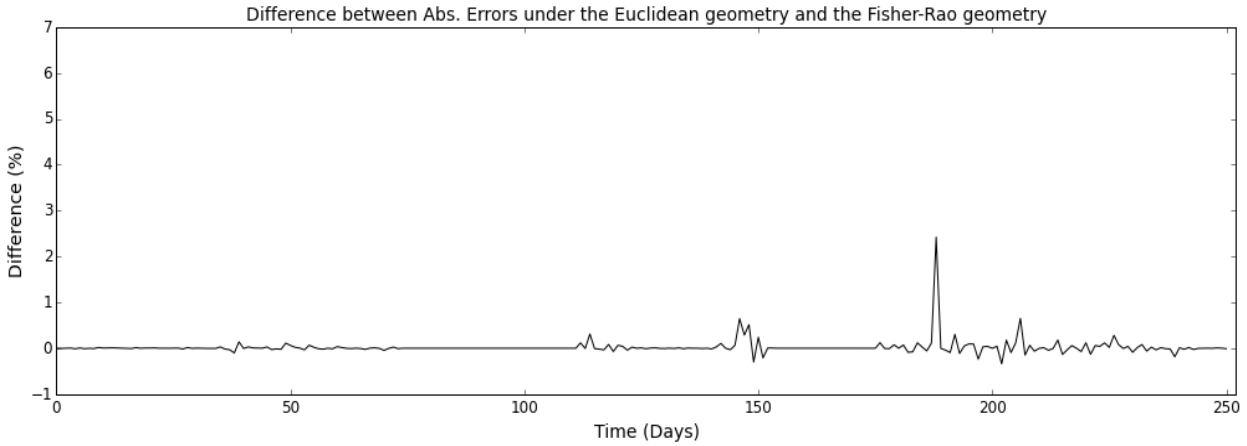

Fig. 8.10. Difference between the absolute approximation errors under the Euclidean geometry and the Riemannian geometry associated with the Fisher–Rao information metric. The initial price of the underlying asset is given by $S_0 = 11.85$ and $S_T = 9.15$ at expiry with fixed $K = 13$.

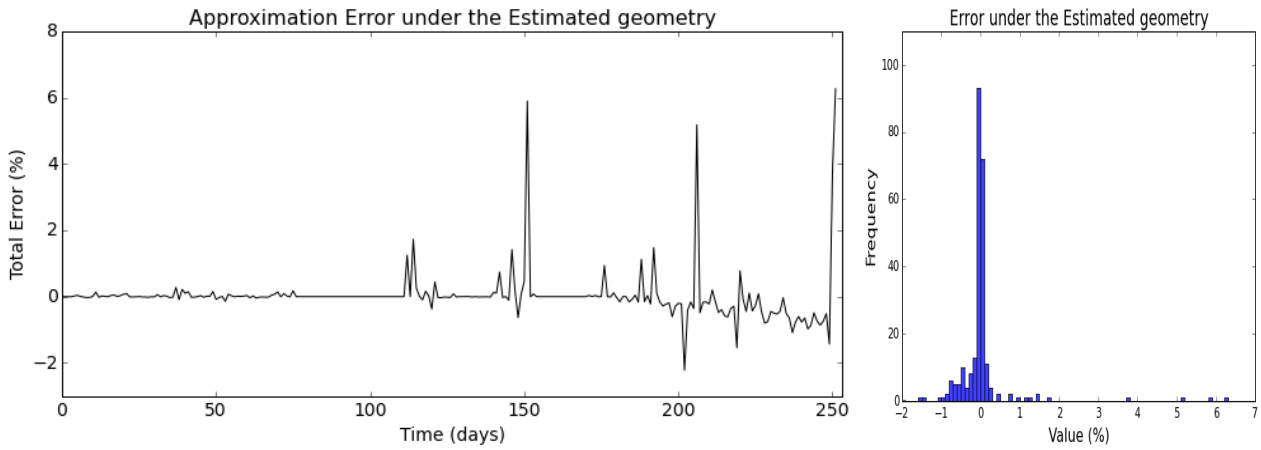

Fig. 8.11. Total approximation errors under the Estimated geometry. The initial price of the underlying asset is given by $S_0 = 11.85$ and $S_T = 9.15$ at expiry with fixed $K = 13$. Descriptive statistics: mean = 0.019%, std. dev. = 0.0077, skew = 5.32.

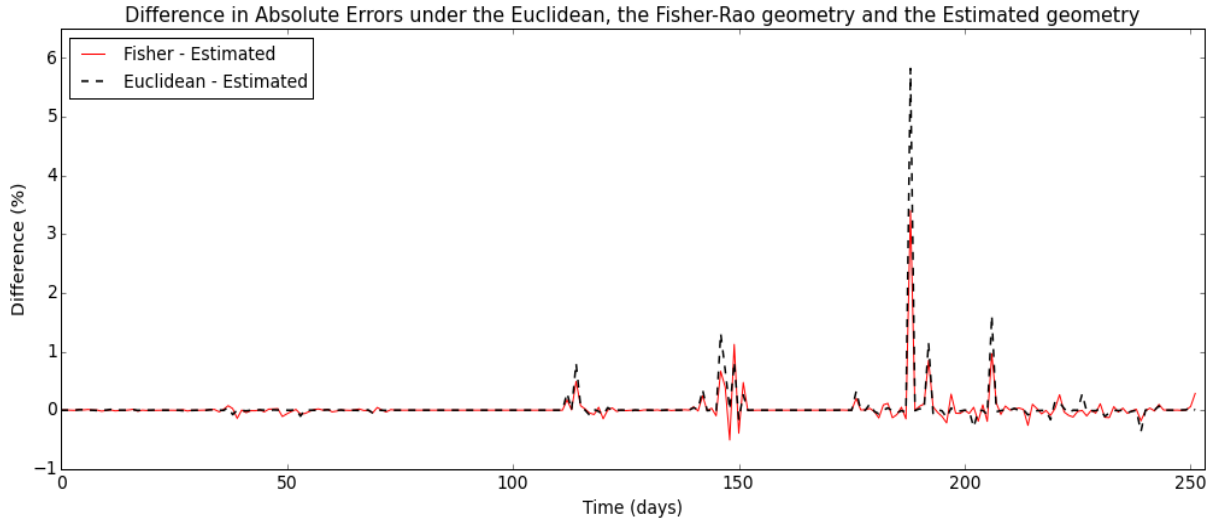

Fig. 8.12. Difference between the absolute approximation errors under the Euclidean geometry, the Riemannian geometry associated with the Fisher–Rao information metric and the Estimated geometry.